Neutron diffraction study and magnetic properties of $La_{1-x}Ba_xCoO_3$ (x = 0.2 and 0.3)

2009 J. Phys.: Condens. Matter 21 156004

(http://iopscience.iop.org/0953-8984/21/15/156004)

J. Phys.: Condens. Matter **21** (2009) 156004 (9pp) doi:10.1088/0953-8984/21/15/156004

Neutron diffraction study and magnetic properties of $La_{1-x}Ba_xCoO_3$ ($x = 0.2$ and 0.3)

A P Sazonov[1,2], I O Troyanchuk[1], H Gamari-Seale[3], V V Sikolenko[4], K L Stefanopoulos[5], G K Nicolaides[6] and Y K Atanassova[6]

[1] SSPA 'Scientific-Practical Materials Research Center of NAS of Belarus', BY-220072 Minsk, Belarus
[2] Institute of Crystallography, RWTH Aachen University, D-52056 Aachen, Germany
[3] Institute of Materials Science, NCSR 'Demokritos', GR-15310 Aghia Paraskevi, Athens, Greece
[4] BENSC, Hahn-Meitner Institut, D-14109 Berlin, Germany
[5] Institute of Physical Chemistry, NCSR 'Demokritos', GR-15310 Aghia Paraskevi, Athens, Greece
[6] Department of Physics, Chemistry and Materials Technology, TEI of Piraeus, GR-12244 Aegaleo, Greece

E-mail: egamari@ims.demokritos.gr

Received 15 September 2008, in final form 3 March 2009
Published 20 March 2009
Online at stacks.iop.org/JPhysCM/21/156004

Abstract

The magnetic properties together with the crystal and magnetic structures of the cobaltites $La_{1-x}Ba_xCoO_3$ (for $x = 0.2$ and 0.3) are determined by DC magnetization, AC magnetic susceptibility and neutron powder diffraction measurements over a broad spectrum of temperatures. For $x = 0.3$ a rhombohedral structure with space group $R\bar{3}c$ is maintained at all temperatures below 300 K. On the other hand, for $x = 0.2$ the refinement of the neutron data below 150 K indicates the coexistence of two structures, $R\bar{3}c$ (rhombohedral) and $Pbnm$ (orthorhombic), respectively, in a ratio of ~48/52. Both compounds ($x = 0.2$ and 0.3) show a ferromagnetic long range order. The data fit well with the Co^{3+} ions in the intermediate spin state and the Co^{4+} ions in a low spin state.

1. Introduction

Rare earth cobaltites with a perovskite structure of the general formula $LnCoO_3$ and their hole-doped $Ln_{1-x}A_xCoO_3$ (Ln = lanthanide, A = divalent element: Ca, Sr or Ba) present a fertile research area for solid state physicists as they exhibit a variety of unusual magnetic and electronic properties. In addition to the lattice, charge and spin degrees of freedom, which are met in many other transition metal oxides, the cobalt oxides will also display a degree of freedom of the 'spin state' of the cobalt site [1–3]. The Co ions in an octahedral symmetry may exhibit either a high, intermediate or low spin state as the energies of the crystal-field splitting of both the Co d states (E_{cf}) and the Hund's rule exchange energy (E_{ex}) are comparable. Thus the Co ions obtain whatever spin state is energetically more favorable. The Co^{3+} low spin state (LS) ($t_{2g}^4e_g^2$, $S = 0$) is energetically more favorable than its high spin state (HS) ($t_{2g}^6e_g^0$, $S = 2$) and might be thermally activated to an intermediate spin state (IS) ($t_{2g}^5e_g^1$, $S = 1$). In the hole-doped cobaltites, $La_{1-x}A_xCoO_3$, the additional Co^{4+} ion increases the complexity of the system as it can also appear with a variety of spin states. Therefore, their electronic and magnetic properties depend on the Co ions' spin states which might differ even in the same sample, resulting in a nanoscale phase separation of the system, leading to a variety of properties as a function of temperature and applied magnetic field. In addition, the ionic size variance of the divalent substitution has been found to affect their properties.

Among doped cobaltites, $La_{1-x}Sr_xCoO_3$ is the most extensively investigated. A spin glass behavior has been revealed for $0.00 \leqslant x \leqslant 0.18$ and a cluster glass behavior

for $0.18 \leqslant x \leqslant 0.50$. For $x > 0.2$, the system transfers to a ferromagnetic long range order. This has also been interpreted as a microscopic phase separation resulting from the non-uniform distribution of Sr. The sample separates into Sr-rich and Sr-poor regions due to the chemical pressure caused by the Sr^{2+} larger ionic radius compared to the ionic radius of La^{3+} and the introduction of holes into the Co–O network [4–15]. According to this interpretation, such a phase separation should be observed for $La_{1-x}Ba_xCoO_3$ as Ba^{2+} has a much larger ionic radius than that of Sr^{2+} [16]. Mandal *et al* [17] have deduced from transport and magnetic measurements that $La_{1-x}Ba_xCoO_3$ shows similarities with $La_{1-x}Sr_xCoO_3$. For $x < 0.2$ the system exhibits a glass-like state dominating the low temperature magnetic properties and a transition takes place from insulator to metal. Kriener *et al* [18] have also shown similarities of the two systems with respect to their magnetic order: $La_{1-x}Ba_xCoO_3$ exhibits lower transition temperatures than the corresponding $La_{1-x}Sr_xCoO_3$, for the same value of x. The system exhibits spin glass behavior for $x < 0.2$ and, above this value, a long range ferromagnetic order is shown. Patil *et al* [19] have reported a ferromagnetic state for $x = 0.2$ with a paramagnetic C–W temperature of 108 K and a magnetic moment of 4.86 μ_B/Co. From electronic and magnetic properties Rao *et al* [20] have deduced a ferromagnetic structure even for $x = 0.1$ at low temperatures with $\theta_p = 100$ K, higher than that of the corresponding composition of the Sr^{2+} or Ca^{2+}. A rhombohedral structure, for $x < 0.35$, at room temperature has been reported while the system transforms to a cubic structure for higher values of x [20–22]. Further, a cubic structure, for $x = 0.3$, is also reported [23]. These compositional structural changes are attributed to the relative high ionic radius of Ba^{2+}. So far there is a broad general agreement for the crystal structure of this cobaltite. The results though for its magnetic state still remain contradictory.

In this work we present the results of DC magnetization, AC magnetic susceptibility measurements and neutron powder diffraction (NPD) experiments on samples of $La_{1-x}Ba_xCoO_3$ (for $x = 0.2$ and 0.3) for a variety of temperatures. Our data indicate that for $x = 0.3$ the crystal structure is rhombohedral (space group $R\bar{3}c$) for the measured range of temperatures 4–300 K. For $x = 0.2$ the NPD data also indicate an $R\bar{3}c$ structure in the temperature range 4–550 K. However, below ~150 K two phases coexist with rhombohedral ($R\bar{3}c$) and orthorhombic ($Pbnm$) structures. A long range ferromagnetic order is maintained at low temperatures for both compounds $La_{1-x}Ba_xCoO_3$ ($x = 0.2$ and 0.3).

2. Experimental procedure

Polycrystalline samples with nominal compositions $La_{0.8}Ba_{0.2}CoO_3$ and $La_{0.7}Ba_{0.3}CoO_3$ were synthesized by the conventional ceramic method. Starting powders of La_2O_3, Co_3O_4 and $BaCoO_3$ were mixed in stoichiometry proportions, pressed into pellets and sintered at 1150 °C for 24 h in air; then the samples were slowly cooled to room temperature at a rate of 50 °C h^{-1}. The neutron powder diffraction (NPD) measurements were performed at the fine-resolution diffractometer E9

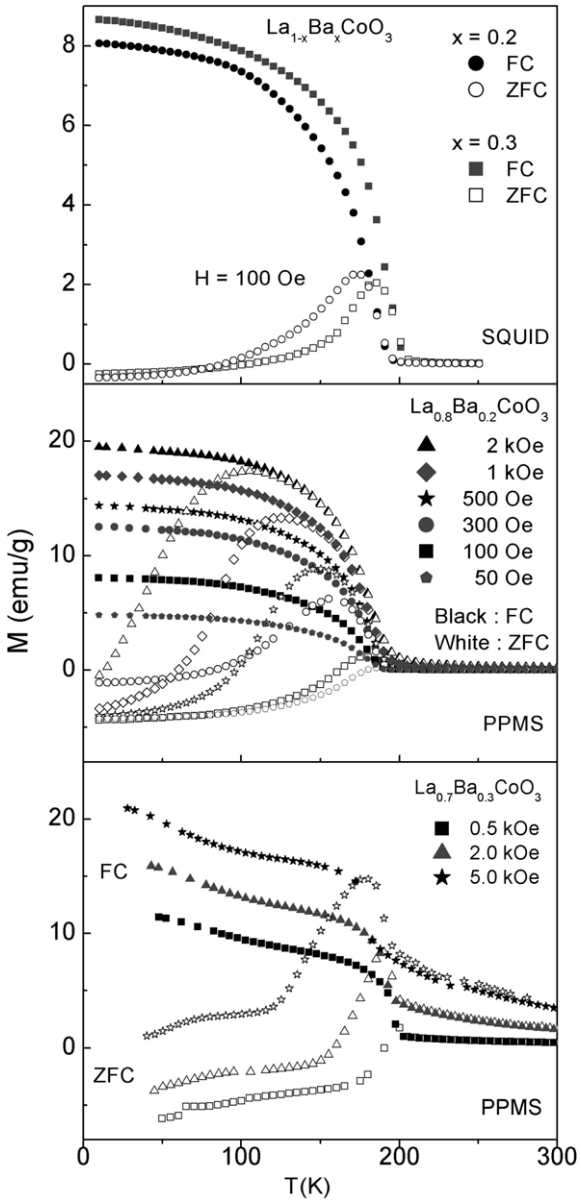

Figure 1. M_{ZFC} and M_{FC} versus T in a variety of applied fields as measured by SQUID, up to 5 T, and PPMS up to 4 kOe, for $La_{1-x}Ba_xCoO_3$ samples ($x = 0.2$, 0.3). The empty symbols are for M_{ZFC} and the solid symbols for M_{FC}.

($\lambda = 1.7973$ Å) installed at the BENSC, HMI, Berlin. Their crystal and magnetic structures were determined for the range of temperatures 4–550 K ($x = 0.2$) and 4–300 K ($x = 0.3$), respectively. This method was also employed to check the purity of the samples and the oxygen deficiency. A small amount of CoO, ~3% and ~1%, for the samples with $x = 0.2$ and 0.3, respectively, was found and was taken into consideration during the refinement of all the experimental data. The oxygen stoichiometry was found to be 3.01(1) and 3.00(2) for $x = 0.2$ and 0.3, respectively. Below their magnetic transition temperature the crystal and magnetic structures were simultaneously refined with the Rietveld method using the FULLPROF program [24].

The intensities of certain reflections with considerable magnetic contributions were also measured at the E1

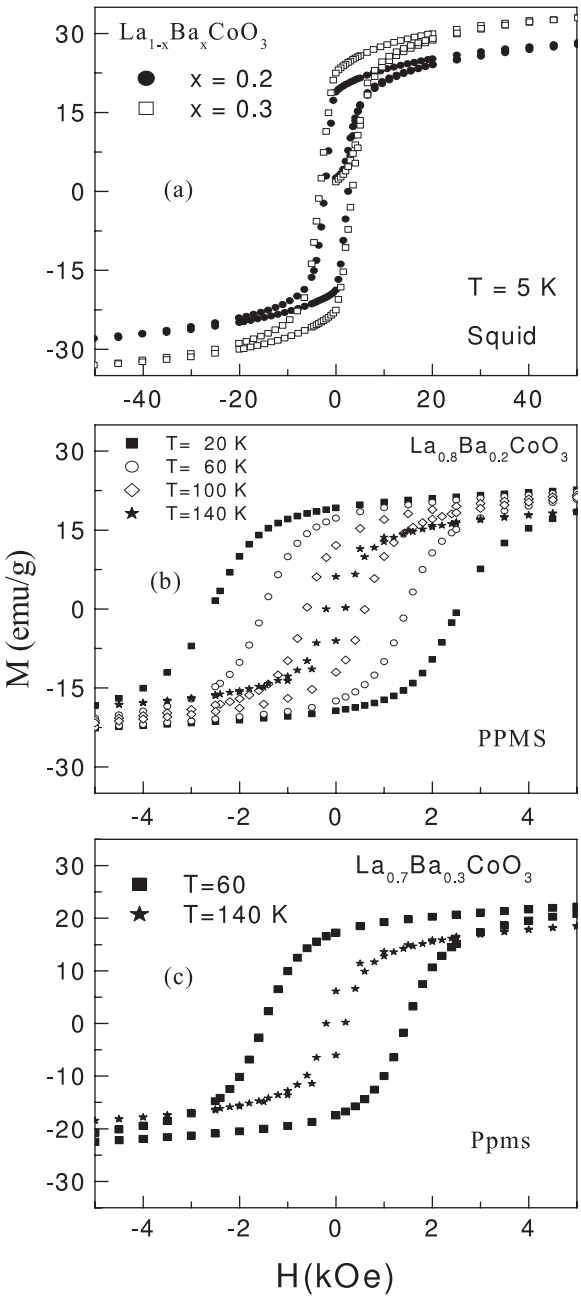

Figure 2. M_{ZFC} versus H at different temperatures for $La_{1-x}Ba_xCoO_3$ samples ($x = 0.2, 0.3$); (a) at 5 K recorded with SQUID; (b) and (c) are recorded with PPMS. The SQUID scale is ten times larger than the scale of PPMS.

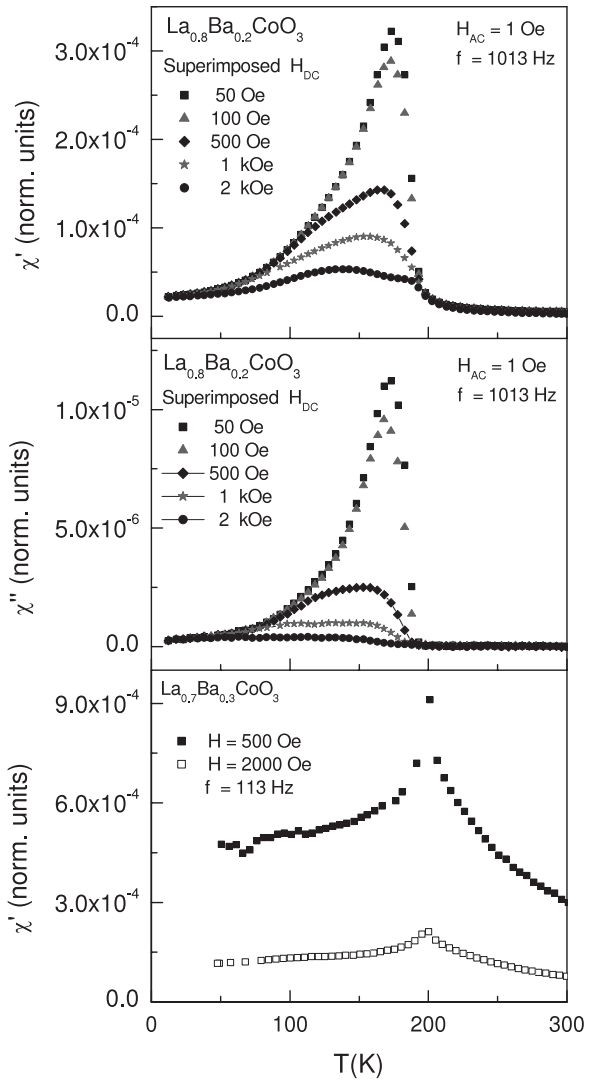

Figure 3. The real part χ' for $La_{1-x}Ba_xCoO_3$ ($x = 0.2, 0.3$) and the imaginary part χ'' for $x = 0.2$ from AC magnetic susceptibility measurements with PPMS.

instrument (HMI) with $\lambda = 2.42$ Å as it is known that the longer wavelengths are particularly useful for investigating magnetic structures.

The macroscopic magnetic properties of the samples were followed from DC magnetization measurements using (a) a SQUID magnetometer, installed at the HMI, by applying a small magnetic field of 100 Oe in the temperature region 4–300 K and (b) by applying different fields in the same temperature region using a Quantum Design PPMS 9T magnetometer, installed at the Technological Education Institute (TEI) of Piraeus. Both the ZFC and the FC modes were applied at all measured temperatures. Hysteresis loops were also recorded at different temperatures. The dynamics of magnetism was studied by the PPMS—AC susceptibility measurements.

3. Results

3.1. Magnetic measurements

Figure 1 shows the temperature dependence of the magnetization for both samples as measured by the two employed apparatuses. The magnetization of both samples exhibits an abrupt increase close to 200 K, slightly higher for $x = 0.3$, which indicates the onset of a long range ferromagnetic order. The corresponding Curie temperatures, T_C, are close to 190 K and 200 K for $x = 0.2$ and 0.3, respectively, in agreement with the published values in [17] and close to the reported value for $x = 0.3$ in [23]. A characteristic strong irreversibility between the ZFC and FC magnetization curves is observed at a

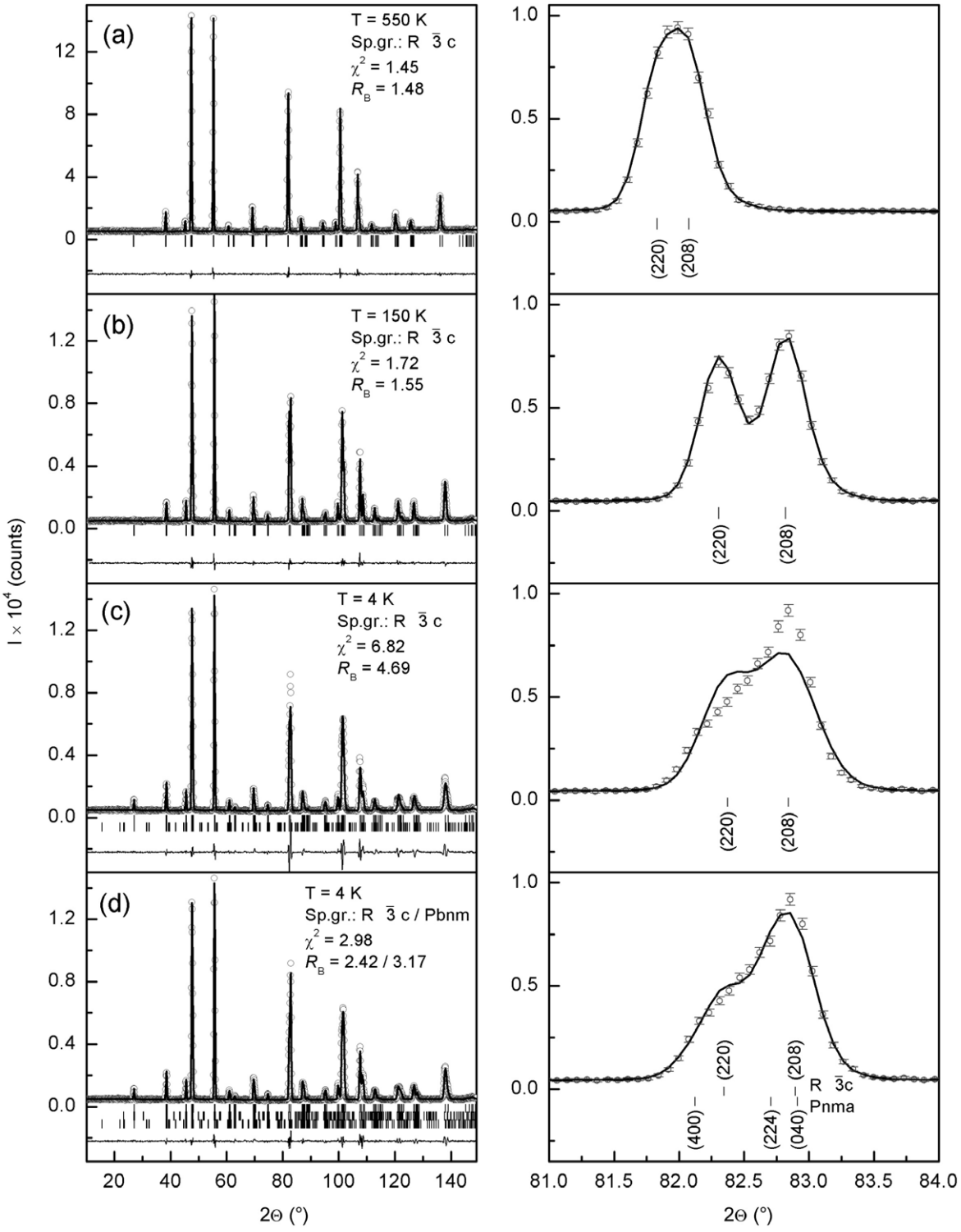

Figure 4. Profile fit of the NPD patterns at selected temperatures for $La_{0.8}Ba_{0.2}CoO_3$. The symbols represent the observed intensities, solid lines represent the calculated patterns, the ticks below mark the calculated reflection positions and the residual curve is shown at the bottom of the figure. An enlarged view of selected reflections at $2\theta \sim 82°$ is also illustrated.

temperature slightly lower than T_C, defined as T_{irr}, decreasing with increasing applied field. At T_{irr} the ZFC curve exhibits a broad maximum and decreases below T_{irr} while the FC magnetization almost flattens as the temperature decreases. Similar irreversibility has also been observed in the system $La_{1-x}Sr_xCoO_3$ [11, 12] and it has been interpreted as the formation of a spin glass or cluster glass state. However, it has been proven that pure ferromagnetic systems can show similar magnetization curves. The gap in temperature between T_{irr} and T_C depends on the relative strength of the applied magnetic field and the magnetocrystalline anisotropy. This feature is symptomatic of ferromagnets with strong anisotropy [25].

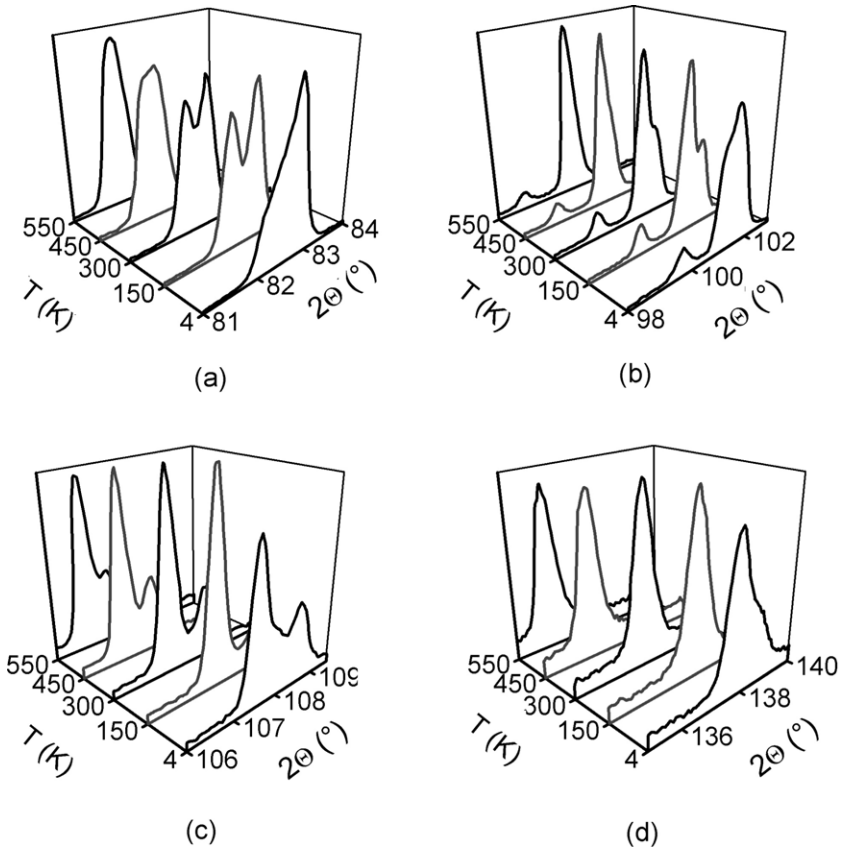

Figure 5. Indicative plots of the changes of the reflection intensities with respect to the angle and the temperature for $La_{0.8}Ba_{0.2}CoO_3$. The corresponding reflections for the rhombohedral phase at different angles are: (a) (208–220), (b) (422), (c) (404–012) and (d) (048).

Similar behavior of the magnetization versus temperature was observed for $La_{0.7}Ba_{0.3}CoO_3$ in an applied field of 3 kOe and it was attributed to ferromagnetic behavior with exchange anisotropy [23].

The negative magnetization observed in the ZFC at low temperatures and in small applied external fields is a result of a remanent field of the superconductive magnet of the instruments used. Even though the field was brought to zero before the sample was cooled down, there is always a remanent field in the vicinity of the sample.

In figure 2 the M versus H curves are plotted at different temperatures up to 140 K. The maximum applied field for the SQUID is ten times higher than that of the PPMS. The increase of the coercive field and the remanent magnetization with decreasing temperature are additional evidence of a long range ferromagnetic order.

The magnetic status of the studied systems is further elucidated by the AC susceptibility data, shown in figure 3. The in-phase component, χ', exhibits a pronounced peak in the vicinity of T_C, which decreases and broadens with increasing field. The same is observed for the out-of-phase χ'' for the sample with $x = 0.2$. For the sample with $x = 0.3$, χ'' is not shown as it was difficult to distinguish it from the background. We found that the position of the peaks is independent of the frequency of the measurements (not shown here), excluding a spin glass state.

The ZFC–FC irreversibility, the increase in the coercive field, the remanent magnetization with decreasing field as well as that the AC susceptibility is independent of the measured frequency strongly suggest a long range ferromagnetic order. With respect to the Curie temperature, our data agree well with those in [17], but they are in disagreement with respect to the derived values of the μ_B/Co ion for $x = 0.2$. Their M versus T curve for $x = 0.2$ in an applied field of 500 Oe lies much below the corresponding one for $x = 0.3$. The resulting magnetic moments are close to 0.65 and 0.33 μ_B/Co for $x = 0.3$ and $x = 0.2$, respectively. Our magnetization measurements in a magnetic field also of 500 Oe give for $x = 0.3$ a value of 0.66 μ_B/Co but 0.55 μ_B/Co for $x = 0.2$. The large difference for $x = 0.2$ is probably due to a compositional difference of the two samples.

In the field of 5 T (figure 2, SQUID technique) the systems does not reach saturation. The derived mean values of the magnetic moments for the Co ions are 1.54 and 1.21 μ_B/Co for $x = 0.3$ and $x = 0.2$, respectively.

3.2. Neutron diffraction

3.2.1. Determination of the crystal structure at different temperatures. Selected diffraction patterns are shown in figures 4 and 6 for both measured samples at different temperatures No broadening of the peaks is observed, thus excluding a nanoscale phase separation, considering at least particles of mesoscopic length scale. The diffraction profile can be refined successfully with a single-phase model in the rhombohedral space group $R\bar{3}c$ in the range 4–300 K for

Table 1. Lattice parameters, atomic coordinates, fractional parameters, reliability factors and magnetic moments μ_{Co} at selected temperatures for $La_{0.8}Ba_{0.2}CoO_3$ as derived from the refinement of the NPD patterns. The structural cell parameters for the $R\bar{3}c$ phase are referred to the hexagonal setting (atomic positions for the $R\bar{3}c$ phase are: La/Ba 6a (0, 0, 1/4), Co 6b (0, 0, 0), O 18e (0, x, 1/4); atomic positions for the $Pbnm$ phase are: La/Ba 4c (x, y, 1/4), Co 4b (1/2, 0, 0), O1 4c (x, y, 1/4), O2 8d (x, y, z)).

T (K)			4	150	300	550
Space group		$R\bar{3}c$	$Pbnm$	$R\bar{3}c$	$R\bar{3}c$	$R\bar{3}c$
Fraction (wt%)		48	52	100	100	100
a (Å)		5.4597(2)	5.4719(2)	5.4620(2)	5.4708(2)	5.4880(1)
b (Å)		5.4597(2)	5.4292(3)	5.4620(2)	5.4708(2)	5.4880(1)
c (Å)		13.2651(3)	7.6790(3)	13.2767(3)	13.3157(3)	13.3934(2)
La/Ba	x	0	0.0006(4)	0	0	0
	y	0	0.0019(3)	0	0	0
	z	0.25	0.25	0.25	0.25	0.25
Co	x	0	0.5	0	0	0
	y	0	0	0	0	0
	z	0.25	0	0.25	0.25	25
O1	x	0	0.0426(2)	0	0	0
	y	0.46891(5)	0.5004(4)	0.46793(2)	0.46963(2)	0.47528(3)
	z	0.25	0.25	0.25	0.25	0.25
O2	x		0.7455(3)			
	y		0.2562(2)			
	z		0.0227(5)			
R_B		2.42	3.17	1.55	1.72	1.48
R_f		2.52	3.55	1.68	2.04	2.03
χ^2			2.98[a]	1.72	1.59	1.45
R_{magn}		6.58	7.04	5.73		
μ_{Co} (μ_B)		1.68(3)	1.68(4)	1.09(3)		

[a] χ^2 is referring to both structures.

$x = 0.3$. On the other hand, for $x = 0.2$ the patterns are successfully fitted with the same $R\bar{3}c$ structure only above 150 K (see figure 4), in agreement with the reported structures in [18–21]. However, below about 150 K, additional splitting of several reflections appears in the diffraction patterns and strong redistribution of peak intensities occurs (figure 5). The neutron diffraction pattern of this sample at 4 K could not be fitted by a simple rhombohedral $R\bar{3}c$ structure, which is confirmed by the splitting of the peak at $2\theta \sim 136°$ (figure 5(d)). Exploratory refinement with the rhombohedral model, used successfully at high temperatures, indicates immediately the presence of more than one phase. This can be seen in figures 4 and 5. Each subfigure of figure 5 represents a combination of several different peaks. With decreasing temperature the rhombohedral distortion is increased. This is clearly seen by the increased separation of the (220) and (208) reflections at 4 K (figure 5(a)). Besides the rhombohedral reflections (200) and (208) below ~150 K, new reflections with similar 2θ appear (figures 4 and 5). Therefore, a two-phase model was employed in the refinement, excluding the low angle reflections in the first step to avoid magnetic contributions, resulting in a successful fitting. After that, the crystal and magnetic structures were refined simultaneously. Due to the rather small overall magnetic contribution to the diffraction patterns the magnetic structure was refined in the single-phase model in contrast to the crystal structure. Thus, the averaged magnetic moment for both rhombohedral and orthorhombic phases was calculated. The best fit was obtained by including in the refinement the rhombohedral ($R\bar{3}c$) and orthorhombic ($Pbnm$) phases in the ratio ~48/52, respectively.

3.2.2. Magnetic structure. The increase in the intensities, especially for the low angle reflections, below a certain temperature for both samples reveals that a ferromagnetic order takes place. No antiferromagnetic contribution has been detected. The average magnetic moments at 4 K obtained from both instruments, E1 and E9, are close to 1.68 μ_B/Co for the sample with $x = 0.2$ and to 1.74 μ_B/Co for $x = 0.3$ (figure 7). These values are slightly higher than those obtained from magnetization measurements at 5 K and in a field of 5 T, namely 1.21 and 1.54 μ_B/Co for $x = 0.2$ and $x = 0.3$, respectively. This indicates that no saturation is achieved in the fields up to 5 T from SQUID measurements. The present experimental results are in agreement with the reported magnetic structure in [18] but only to the type of magnetic ordering. Tables 1 and 2 show the data obtained from the refinement of the NPD data.

3.2.3. Temperature variation of the structural parameters. The temperature variation of the lattice parameters, the unit cell volumes, the bond lengths and the angles as deduced from the refinement of the NPD patterns are presented in figure 8. The lattice parameters are shown in the perovskite-like pseudo-cell settings ($a_p = a_r/\sqrt{2}$, $c_p = c_r/\sqrt{12}$, $V_p = V_r/6$). All parameters exhibit a regular thermal expansion, indicating no abnormal structural changes with decreasing temperature. For $x = 0.2$, the calculations are made only for the rhombohedral

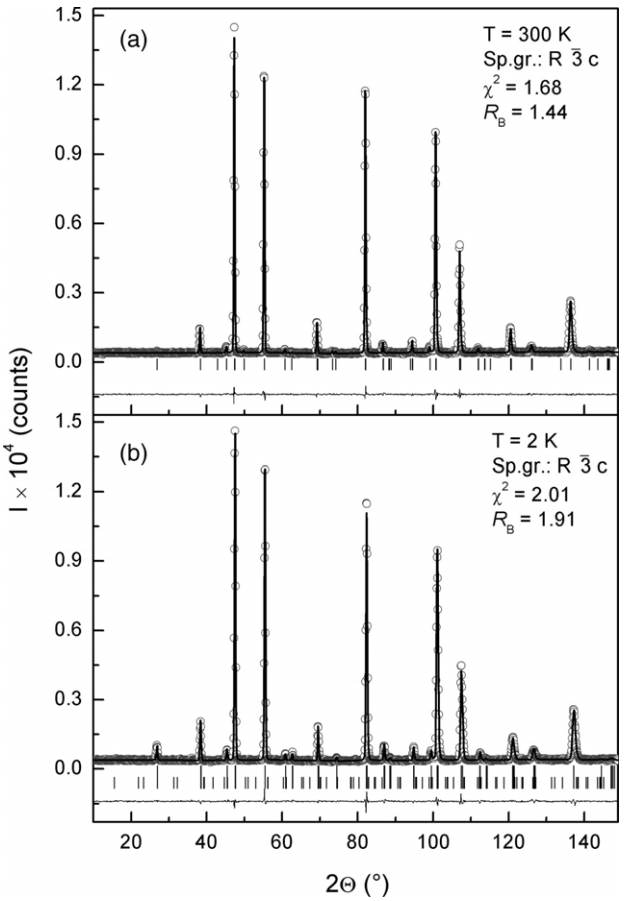

Figure 6. Profile fit of the NPD patterns at selected temperatures for $La_{0.7}Ba_{0.3}CoO_3$. The symbols represent the observed intensities, solid lines represent the calculated patterns, the ticks below mark the calculated reflection positions and the residual curve is shown at the bottom of the figure.

structure as we do not have data for a variety of temperatures in the case of the orthorhombic structure. The increase of the cell volume with increasing x is attributed to the higher ionic radius of Ba^{2+} in comparison with the La^{3+} ionic radius. For $x = 0.2$, there is a perfect agreement with the results of [21]. For $x = 0.3$, there are some small discrepancies, although the general trend is the same. Regular changes are also observed for the Co–O bond lengths and the Co–O–Co angle. The bond lengths for both samples are in between the sum of the ionic radii of Co^{3+} in the HS state and Co^{3+} in the LS state (1.95 and 1.89, respectively [15]) and the oxygen, excluding the possibility of the LS or HS state in a pure ionic model.

A rhombohedral distortion is attributed to the cooperative rotation of the CoO_6 polyhedra about the threefold axis of the ideal cubic perovskites. The departure from 180° of the Co–O–Co angle modulates the strength of the Co–O–Co interaction and affects the magnetic transition temperature. Our data gives less deviation for $x = 0.3$, justifying the slightly higher magnetic transition temperature and suggesting that the system has a tendency to cubic structure for higher values of x, as has been reported in [19–21].

3.2.4. Determination of the spin state of Co ions, ferromagnetic order. The Co spin states can be deduced from the

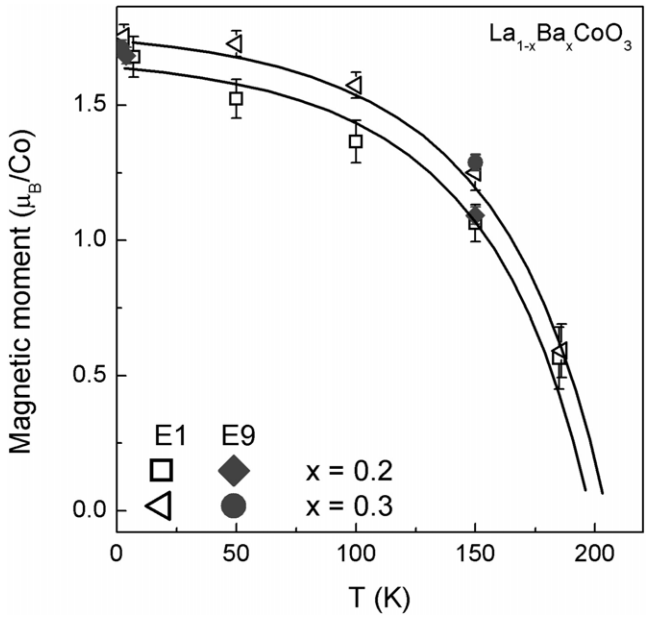

Figure 7. The magnetic moments for the $La_{1-x}Ba_xCoO_3$ samples ($x = 0.2, 0.3$) as derived from the NPD refinements from both E9 and E1 instruments.

Table 2. Lattice parameters, atomic coordinates, fractional parameters, reliability factors and magnetic moments μ_{Co} as derived from the refinement of the NPD patterns for $La_{0.7}Ba_{0.3}CoO_3$; space group $R\bar{3}c$. The cell parameters and the atomic coordinates are referred to the hexagonal setting (atomic positions: La/Ba 6a (0, 0, 1/4), Co 6b (0, 0, 0) and O 18e (0, x, 1/4)).

T (K)		2	150	300
a, b (Å)		5.4629(3)	5.4665(3)	5.4761(4)
c (Å)		13.3487(4)	13.355(3)	13.3932(3)
La/Ba	x	0	0	0
	y	0	0	0
	z	0.25	0.25	0.25
Co	x	0	0	0
	y	0	0	0
	z	0	0	0
O	x	0	0	0
	y	0.47826(3)	0.46809(4)	0.48395(4)
	z	0.25	0.25	0.25
R_B		1.91	1.64	1.44
R_f		2.63	2.22	2.01
χ^2		2.01	1.98	1.68
R_{magn}		4.00	4.53	
μ_{Co} (μ_B)		1.75(3)	1.29(3)	

experimental values of the magnetic moments. As deduced from the stoichiometry the ratio Co^{3+}/Co^{4+} is respectively 4 for $x = 0.2$, and 2.5 for $x = 0.3$. The experimentally deduced magnetic moments are 1.68 and 1.74 μ_B/Co, respectively, fitting with the Co^{3+} being in the intermediate spin state ($t_{2g}^5 e_g^1$, $S = 1$), as has been deduced as well from the bond lengths, and with the Co^{4+} in a low spin state ($t_{2g}^5 e_g^0$, $S = 1/2$) by applying a pure ionic model. Any other spin states are excluded, as the calculated magnetic moments are much higher than the experimentally deduced ones. Similar values

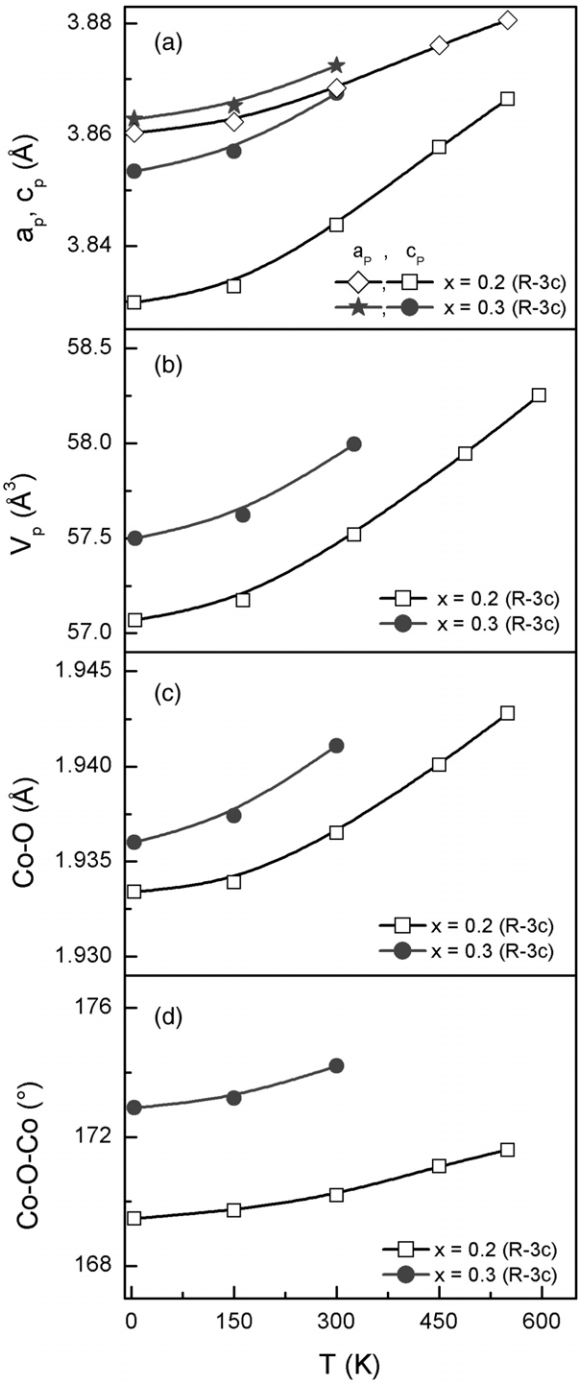

Figure 8. The cell parameters and volume, the bond lengths and bond angles with respect to temperature for $La_{1-x}Ba_xCoO_3$ ($x = 0.2, 0.3$) as derived from the NPD refinement.

of magnetic moments have also been found for $La_{1-x}Sr_xCoO_3$ experimentally and from theoretical calculations as well [26]. Hole doping with Ba introduces Co^{4+} in LS which stabilizes the IS Co^{3+} in the neighbors, as has been found by neutron diffraction experiments for $La_{1-x}Sr_xCoO_3$ [11]. The ferromagnetic order follows the superexchange mechanism by the e_g electron hopping between the Co sites or it is caused by itinerant electrons [27]. The large magnetic moments reported by Patil *et al* [19] derived from the paramagnetic region can only be accounted for by assuming that both ions are in the HS state, which is in disagreement with those deduced from our NPD data. In our opinion, their high values of the magnetic moments are probably due to the fact that they have been derived from the paramagnetic region at 300 K, a temperature close to the ordering temperature which is known to include large errors.

4. Discussion and conclusions

The macroscopic phase separation observed in the sample with $x = 0.2$ below a certain temperature is not a peculiarity of this system. Various materials have been reported to display a single diffraction pattern at high temperature and, below a certain temperature, a variety of phases [28–32]. Low temperature macroscopic phase coexistence/separation is usually attributed to chemical heterogeneity of the sample containing domains or particles with slightly different electronic concentrations. The domains with slightly different chemical compositions undergo different thermal evolution. At room temperature, only one phase is observed. At the transition temperature, the phase coexistence comes into sight. A possible scenario is that, when the structural transition takes place, large strains may develop between the nucleation centers and the pristine material which prohibit transformation of the total sample volume.

The present data resemble those obtained for $La_{0.8}Ba_{0.2}MnO_3$. X-ray measurements on single crystals of $La_{0.8}Ba_{0.2}MnO_3$ by Gaviko *et al* [33] for a broad spectrum of temperatures suggested that the compound is of a single phase $R\bar{3}c$ at 196 K and a single orthorhombic $Pbnm$ at lower temperatures. In the interval 185–196 K both phases were detected. This interval increases for lower values of Ba content and decreases as the Ba content increases. Dabrowski *et al* [34] performed neutron diffraction experiments on polycrystalline samples of $La_{1-x}Ba_xMnO_3$ ($x = 0.10$–0.24). They concluded that the sample with $x = 0.12$ was two-phase, 97% $Pbnm$ and 3% $R\bar{3}c$. Similarly, the present data on $La_{0.8}Ba_{0.2}CoO_3$ indicate only the $R\bar{3}c$ structure above 150 K and a phase transformation starting at about 150 K as the temperature decreases. At 4 K both structures $R\bar{3}c$ and $Pbnm$ still coexist.

If the low temperature coexistence of the two phases for $La_{0.8}Ba_{0.2}CoO_3$ is related to preexisting heterogeneity of the A-site cations, which is very common in the perovskites, due to inadequate sample preparation, all phases should also be present at high temperatures. The high temperature patterns for $La_{0.8}Ba_{0.2}CoO_3$ fit extremely well with the $R\bar{3}c$ structure, suggested by the low reliability factors. If we assume that the A-site cations are randomly distributed, only a single phase, $R\bar{3}c$, at high temperature should be present, as has been observed in our case. We believe that the sample should transform to the orthorhombic $Pbnm$ structure as in the case of $La_{0..8}Ba_{0.2}MnO_3$. However, the complete transformation is prevented by large strains developed between the nucleation centers and the pristine material prohibiting the complete sample volume transformation in an analogous fashion to the mechanism of martensitic phase transitions where metastable unchanged domains coexist with the stable transformed phase.

In conclusion, DC magnetization, AC magnetic susceptibility and neutron diffraction measurements on both $La_{0.8}Ba_{0.2}CoO_3$ and $La_{0.7}Ba_{0.3}CoO_3$ cobaltites revealed a long range ferromagnetic order. The experimental Co magnetic moment values for both samples are in good agreement with the Co^{3+} being in the IS state and the Co^{4+} in the LS state. The ferromagnetic order is established due to the positive interactions between the Co^{3+} and Co^{4+} ions which interact via the oxygen p orbital. NPD data indicate a rhombohedral structure $R\bar{3}c$ at all temperatures for $x = 0.3$. On the other hand, for $x = 0.2$ a single phase with the same rhombohedral structure $R\bar{3}c$ is determined in the temperature range 150–500 K. Below 150 K, however, the NPD data indicate the coexistence of the $R\bar{3}c$ phase and the orthorhombic $Pbnm$ in a ratio of ∼48/52.

Acknowledgments

This research project has been partly supported by the European Commission under the 6th Framework Program through the Key Action: Strengthening the European Research Area, Research Infrastructures, contract no. RII3-CT-2003-505925 (NMI3).

References

[1] Imada M, Arima A, Fujimori A and Tokura Y 1998 *Rev. Mod. Phys.* **70** 1039
[2] Asai K, Ghering P, Chou H and Shirane G 1989 *Phys. Rev.* B **40** 10982
[3] Yamaguchi S, Okimoto Y and Tokura Y 1997 *Phys. Rev.* B **55** R8666
[4] Nam D N H, Jonason K, Nordblad P, Khiem N V and Phuc N X 1999 *Phys. Rev.* B **59** 4189
[5] Phuc X, Khiem N V and Nam D N H 2002 *J. Magn. Magn. Mater.* **242–245** 754
[6] Mukherjiee S, Ranganathan R, Anikumar P S and Joy P A 1996 *Phys. Rev.* B **54** 9267
[7] Itoch M, Natori I, Kubota S and Motoya K J 1995 *J. Magn. Magn. Mater.* **140–144** 1811
[8] Asai K, Yokomoura O, Nishimori N, Chou H, Tranquada J M, Shirane G, Higuc S, Okajyma Y and Kohn K 1994 *Phys. Rev.* B **50** 3025
[9] Senaris M A and Goodenough J B 1995 *J. Solid State Chem.* **118** 323
[10] Asai K, Yoneda A, Yokokura O, Tranquada J M, Shirane G and Kohn K 1998 *J. Phys. Soc. Japan* **67** 290
[11] Cacioufo R, Rinaldi D, Barucca C, Mira J Rivas J, Senaris-Rodrighez S A, Fiorani D and Goodenough J B 1999-II *Phys. Rev.* B **59** 1068
[12] Wu J and Leighton C 2003 *Phys. Rev.* B **67** 174408
[13] Nam D N H, Mathieu R, Nordmlad P, Khiem N V K and Phuc N X 2000-I *Phys. Rev.* B **62** 8989
[14] Hoch M R J, Kuhns P L, Moulton W G, Reyes A P, Lu J, Wu J and Leighton C 2004 *Phys. Rev.* B **70** 174443
[15] Phan T L, Oh S K, Bau L B, Phuc N X and Yu S C J 2006 *J. Magn. Magn. Mater.* **300** e183
[16] Shannon R D 1976 *Acta Crystallogr.* A **32** 751
[17] Mandal P, Choudhury P, Biswas S K and Ghosh B 2004 *Phys. Rev.* B **70** 104407
[18] Kriener M, Zobel C, Reichl A, Baier J, Cwick M, Berggold K, Kierspel H, Zabara O, Freimuth A and Lorenz T 2004 *Phys. Rev.* B **69** 094417
[19] Patil S B, Meer H V and Chakrabarty D K 1978 *Phys. Status Solidi* a **52** 681
[20] Rao C N R, Parkash O, Barkash D, Bahadur D, Ganguly P and Nagashushama S 1997 *J. Solid State Chem.* **23** 353
[21] Luo W and Wang F 2006 *Powder Diffr.* **21** 304
[22] Fauth F, Shuard E and Caignart V 2001 *Phys. Rev.* B **65** 060401(R)
[23] Ganfguly R, Gopalakrishnan I K and Yakhmi J V 1999 *Physica* B **271** 116
[24] Rodríguez-Carvajal J 1993 *Physica* B **192** 55
[25] Kumar P S, Joy P A and Date S K 1998 *J. Appl. Phys.* **83** 7375
Kumar P S, Joy P A and Date S K 1998 *J. Phys.: Condens. Matter* **10** 487
[26] Ravinndran R, Fjellvag H, Kjekshus A, Blada P, Schawartz K and Luitz J 2002 *J. Appl. Phys.* **91** 291
[27] Sazonov A P, Troyanchuk I O, Sikolenko V V, Chobot G M and Szymczak H 2005 *J. Phys.: Condens. Matter* **17** 4181
[28] Ritter C, Radaelli P G, Balakrishan J and Paul M D K 1996 *J. Solid State Chem.* **127** 276
[29] Damay F, Martin C, Hervieu M, Maignam M, Raveau B, Andre G and Bouree F 1998 *J. Magn. Magn. Mater.* **184** 71
[30] Arulraj A, Biswas A, Raychaudhuri A K, Rao C N R, Woodward P M, Vogt T, Cox D E and Cheetham A K 1998 *Phys. Rev.* B **57** R8185
[31] Rhyne J J, Kaiser H, Luo H, Xiao G and Gardel M L 1998 *J. Appl. Phys.* **83** 7339
[32] Martin C, Maignam A, Hervieu M, Raveau B, Jirak Z, Kurbakov A, Trounov B, Andre C and Bouree F 1999 *J. Magn. Magn. Mater.* **205** 184
[33] Gaviko V S, Bebenin N G and Mukovskii Y M 2008 *Phys. Rev.* B **77** 224105
[34] Dabrowski B, Rogacki K, Xiong X, Klamut P W, Dybzinski R, Shaffer J and Jorgensen J D 1998 *Phys. Rev.* B **58** 2716